JOURNAL OF SOLID STATE CHEMISTRY 115, 360–367 (1995)

Crystal Structure and Polarized Electronic Absorption Spectra of $NaCo_2(SeO_3)_2(OH)$

M. Wildner[1]

Institut für Mineralogie und Kristallographie, Technische Universität Berlin, Ernst-Reuter-Platz 1, D-10587 Berlin, Germany

Received June 10, 1994; accepted August 11, 1994

The crystal structure of hydrothermally synthesized $NaCo_2(SeO_3)_2(OH)$ has been determined by direct and Fourier methods using single crystal X-ray diffraction data up to $\sin\theta/\lambda = 0.8$ Å^{-1} [orthorhombic, space group *Pbnm*, $a = 8.338(1)$ Å, $b = 13.268(3)$ Å, $c = 6.042(1)$ Å, $Z = 4$; $R_w = 0.023$ for 1407 unique reflections with $F_o > 2\sigma(F_o)$]. The structure of $NaCo_2(SeO_3)_2(OH)$ consists of [4 + 2]-coordinated Na atoms, distorted CoO_6 octahedra, pyramidal SeO_3 groups, and hydroxyl groups. The CoO_6 polyhedra form $^1_\infty[Co_4O_{14}]^{20-}$ zigzag chains, analogous to the respective Me^{2+} chains in the olivine structure type. These chains are connected via the selenite groups and sodium atoms. The O atom of the hydroxyl group belongs to three CoO_6 polyhedra and forms a bifurcated hydrogen bond (3.312 Å, 2×). Furthermore, polarized electronic absorption spectra of $NaCo_2(SeO_3)_2(OH)$ have been measured in the range from 4000 to 40,000 cm^{-1} using microscope spectrometric techniques. The spectra are characterized by electric dipole transitions at the acentric Co^{2+} site [Co(2)]. An interpretation of the band splitting and polarization behavior is attempted in terms of a pseudotetragonal field component and the imposed actual monoclinic site perturbation, yielding $^4A_2(F)$ and $^4A''(F)$ as respective ground states. Tetragonal crystal field calculations give $Dq = 630$, $Dt = -135$, $Ds = -111$, $B = 843$, and $C = 3520$ cm^{-1}, which corresponds to a "cubic" Dq of 709 cm^{-1}. The sign and magnitude of the tetragonal parameter Dt is in good agreement with the pseudotetragonal compression of the $Co(2)O_6$ polyhedron.

INTRODUCTION

In the system CoO–SeO_2–(H_2O), a small number of compounds have been structurally characterized up to now, namely, $CoSeO_3$ (1), $CoSeO_3 \cdot 2H_2O$ (2, 3), $Co_3(SeO_3)_3 \cdot H_2O$ (4), and $CoSe_2O_5$ (5, 6). The same is true for the inclusion of alkali elements into this system, since so far only the structures of $K_2Co(SeO_3)_2$ (7), $K_2Co_2(SeO_3)_3$ (8), and $K_2[Co_2(SeO_3)_3] \cdot 2H_2O$ (9) have been determined. They exhibit some remarkable structural features: $K_2Co(SeO_3)_2$ represents the first example for isotypism of a selenite with a carbonate, i.e., $K_2Ca(CO_3)_2$ (buetschliite); the structure of $K_2Co_2(SeO_3)_3$ is very closely related to $K_2Co(SeO_3)_2$. $K_2[Co_2(SeO_3)_3] \cdot 2H_2O$ belongs to the zemannite-type compounds, forming a microporous structure containing wide channels within a honeycomb-like $[Co_2(SeO_3)_3]^{2-}$ framework.

In the present paper the synthesis, crystal structure, and polarized electronic absorption spectra of the first Na representative within this system, $NaCo_2(SeO_3)_2(OH)$, are reported. For a preliminary note on the structure of this compound, see (10).

EXPERIMENTAL

Single crystals of $NaCo_2(SeO_3)_2(OH)$ were prepared under hydrothermal conditions. An appropriate mixture of $Co(OH)_2$, $NaHCO_3$, and H_2SeO_4 was inserted in a Teflon-lined steel vessel ($V \sim 4$ ml) and some drops of water were added. The closed vessel was kept at a temperature of ~485 K for 4 days. The crystals, obtained in sizes up to 0.3 mm, form plates that are parallel to (010) and/or elongated along c. $NaCo_2(SeO_3)_2(OH)$ crystallizes in space group *Pbnm* (No. 62); the space group setting was chosen according to $c < a < b$ recommended by (11). Lattice parameters (refined from 40 accurate 2θ values in the range $32° < 2\theta < 42°$) and X-ray diffraction data up to $2\theta = 70°$ were measured on a Stoe four-circle AED2 diffractometer using graphite-monochromatized Mo$K\alpha$ radiation (2θ-ω scans; 40 steps/reflection, increased for α_1–α_2 splitting; 0.03° and 0.5–1.5 sec/step; 2 × 6 steps for background measurements; three standard reflections each 120 min). Corrections for Lorentz and polarization effects, as well as an empirical correction for absorption effects (Ψ-scans), were applied. Complex scattering curves were taken from (12). Details of the structure refinement and a summary of crystal data are given in Table 1. The positions of the Co and Se atoms were found by direct methods, the Na and O atoms by Fourier summations. The H atom was located in a subsequent difference Fourier summation and refined isotropically. The final atomic coordinates and anisotropic displacement parame-

[1] Permanent address: Institut für Mineralogie und Kristallographie, Universität Wien, Dr. Karl Lueger-Ring 1, A-1010 Vienna, Austria.

0022-4596/95 $6.00

TABLE 1
Summary of Crystal Data, X-Ray Measurements, and Structure Refinement of $NaCo_2(SeO_3)_2(OH)$

Space group	*Pbnm* (No. 62)
a(Å)	8.338(1)
b(Å)	13.268(3)
c(Å)	6.042(1)
V(Å^3)	668.4
Z	4
ρ_{calc}(g cm^{-3})	4.092
μ(Mo$K\alpha$) (cm^{-1})	154.6
Crystal dimensions (mm)	0.3 × 0.1 × 0.1
Extinction coefficient (g) (Ref. 29)	6.2(4) × 10^{-6}
Measured reflections	3227
Unique data set	1592
Data with $F_o > 2\sigma(F_o)$	1407
Variables	71
Transmission factors (Ψ-scans)	0.16–0.25
R	0.026
R_w ($w = 1/[\sigma(F_o)]^2$)	0.023
R (all unique data)	0.034

ters, obtained by full-matrix least-squares refinement, are listed in Table 2. For all calculations the program system STRUCSY (13) was used.

Crystals of $NaCo_2(SeO_3)_2(OH)$ have a dark violet color. In polarized light, they exhibit strong pleochroism: violet-gray, bright lavender, and intense purple when the electric light vector runs parallel to the a, b, and c axes, respectively. The strong absorption in the visible region hampers the determination of optical constants and character. A conoscopic investigation of a (010) plate indicated that (010) is the optical axis plane. The indices of refraction within this plane, n_α and n_γ, were determined by the immersion method using a Jelley–Leitz refractometer parallel to the a axis as 1.795 (433 nm), 1.782 (498 nm), 1.773 (586 nm), and 1.771 (649 nm), parallel to the c axis as 1.811 (due to problems with strong absorption and immersion liquids it was only measured at 586 nm). Therefore, the following orientation of the optical indicatrix can be established: $\alpha \| a$, $\beta \| b$, $\gamma \| c$.

Polarized optical absorption spectra of $NaCo_2(SeO_3)_2(OH)$ were measured on a Zeiss UMSP80 microscope–spectrometer in the range 40,000–4000 cm^{-1}. For details of microscopic–spectrometric techniques, see (14). Two crystals of $NaCo_2(SeO_3)_2(OH)$ were oriented by X-ray oscillation photographs parallel to the a (crystal I) and b (crystal II) axis, embedded together with quartz platelets in epoxy resin, and ground and polished from both sides to 38 μm (I) and 142 μm (II). Thicknesses were determined from the retardation of the quartz platelets as outlined in (15). Absorption spectra β and γ were obtained from crystal slab I, whereas the α spectrum, exhibiting much weaker absorption, was measured with the thicker crystal slab II. Spectral band and step widths were both 1 nm in the UV–Vis region down to 12,000 cm^{-1}, and 10 nm in the NIR region.

Crystal field calculations for the tetragonal field component at the acentric Co(2) site in terms of the parameters Dq, Dt, Ds, and Racah B and C, were performed in two steps. First, Dq, Dt, Ds, and B were fitted by least-squares methods to the spin-allowed transitions using our own program (Wildner, unpublished). This program is based on energy matrices given in the literature (16), but uses inverted signs of Dt and Ds to be consistent with the common sign convention reported by Ballhausen (17). Second, the fitted parameters were used as input values for the Crystal Field Computer Package by Yeung and Rudowicz (18), where calculated spin-forbidden transitions were adjusted to the observed ones by manual variation of the Racah C input value. Spin–orbit coupling was neglected in the calculations.

TABLE 2
Atomic Coordinates and Anisotropic Displacement Parameters (pm^2) in $NaCo_2(SeO_3)_2(OH)$

	x	y	z	$U_{11/iso}$	U_{22}	U_{33}	U_{12}	U_{13}	U_{23}
Na	0.3719(2)	0.7486(1)	¾	206(8)	223(8)	236(7)	25(7)	0	0
Co(1)	0	0	0	121(2)	135(2)	121(2)	−8(2)	−8(2)	0(1)
Co(2)	0.28762(6)	0.11291(4)	¼	114(2)	132(2)	148(2)	−4(2)	0	0
Se(1)	0.27515(5)	0.32935(3)	¼	126(2)	121(2)	198(2)	−4(1)	0	0
Se(2)	0.37988(5)	0.02516(3)	¾	98(1)	139(1)	138(1)	−6(1)	0	0
O(1)	0.9566(3)	0.1091(2)	¾	144(12)	121(11)	164(11)	25(9)	0	0
O(2)	0.5316(4)	0.0887(2)	¼	110(12)	188(12)	320(15)	34(10)	0	0
O(3)	0.8047(3)	0.2542(2)	0.9586(3)	271(11)	173(8)	205(9)	2(8)	34(8)	−22(7)
O(4)	0.2529(2)	0.0149(2)	0.9702(3)	141(8)	217(10)	148(7)	−6(7)	19(7)	−34(6)
O(h)	0.4626(3)	0.6015(2)	¼	134(11)	130(11)	154(11)	−3(9)	0	0
H	0.518(8)	0.665(5)	¼	334(157)					

Note. The anisotropic displacement parameter is defined as $\exp(-2\pi^2\Sigma_i\Sigma_j U_{ij} h_i h_j a_i^* a_j^*)$.

TABLE 3
Interatomic Distances (Å), Bond Angles (°) and Octahedral Distortion Parameters Δ_{oct} $\{=(1/6)\Sigma[(d_i - d_m)/d_m]^2\}$ and σ^2_{oct} $\{=(1/11)\Sigma(a_i - 90°)^2\}$ in $NaCo_2(SeO_3)_2(OH)$

Na	O(1)	O(2)	O(3)	O(3)	[O(3)]	[O(3)]
O(1)	*2.338(3)*	4.058(4)	3.848(3)	3.848(3)	2.627(3)	2.627(3)
O(2)	121.9(1)	*2.304(3)*	3.621(3)	3.621(3)	3.084(3)	3.084(3)
O(3)	112.3(1)	103.8(1)	*2.295(2)*	3.521(4)	4.200(5)	5.150(4)
O(3)	112.3(1)	103.8(1)	100.1(1)	*2.295(2)*	5.150(4)	4.200(5)
[O(3)]	57.8(1)	70.1(1)	104.9(1)	155.0(2)	*2.977(2)*	2.521(4)
[O(3)]	57.8(1)	70.1(1)	155.0(2)	104.9(1)	50.1(2)	*2.977(2)*

$\langle Na^{[4]}–O\rangle$ = *2.308*, $\langle Na^{[6]}–O\rangle$ = *2.531*; $\langle O–Na^{[4]}–O\rangle$ = 109.0

Co(1)	O(1)	O(1)	O(4)	O(4)	O(h)	O(h)
O(1)	*2.123(1)*		3.071(3)	2.936(3)	3.097(1)	2.795(3)
O(1)	180	*2.123(1)*	2.936(3)	3.071(3)	2.795(3)	3.097(1)
O(4)	92.6(1)	87.4(1)	*2.126(2)*		2.722(3)	3.165(3)
O(4)	87.4(1)	92.6(1)	180	*2.126(2)*	3.165(3)	2.722(3)
O(h)	95.9(1)	84.1(1)	81.4(1)	98.6(1)	*2.048(1)*	
O(h)	84.1(1)	95.9(1)	98.6(1)	81.4(1)	180	*2.048(1)*

$\langle Co(1)–O\rangle$ = *2.099*; Δ_{oct} = 0.00030, σ^2_{oct} = 41.9

Co(2)	O(2)	O(3)	O(3)	O(4)	O(4)	O(h)
O(2)	*2.059(3)*	3.084(3)	3.084(3)	3.036(3)	3.036(3)	
O(3)	93.6(1)	*2.172(2)*	2.521(4)	3.123(3)		3.197(3)
O(3)	93.6(1)	71.0(1)	*2.172(2)*		3.123(3)	3.197(3)
O(4)	92.2(1)	92.5(1)	162.8(2)	*2.152(2)*	3.382(4)	2.722(3)
O(4)	92.2(1)	162.8(2)	92.5(1)	103.5(1)	*2.152(2)*	2.722(3)
O(h)	166.9(3)	97.1(1)	97.1(1)	79.8(1)	79.8(1)	*2.092(2)*

$\langle Co(2)–O\rangle$ = *2.133*; Δ_{oct} = 0.00040, σ^2_{oct} = 82.1

Se(1)	O(1)	O(3)	O(3)
O(1)	*1.719(2)*	2.627(3)	2.627(3)
O(3)	100.5(1)	*1.697(1)*	2.521(4)
O(3)	100.5(1)	96.0(1)	*1.697(1)*

$\langle Se(1)–O\rangle$ = *1.704*; $\langle O–Se(1)–O\rangle$ = 99.0

Se(2)	O(2)	O(4)	O(4)
O(2)	*1.681(2)*	2.625(3)	2.625(3)
O(4)	101.6(1)	*1.706(1)*	2.661(4)
O(4)	101.6(1)	102.5(1)	*1.706(1)*

$\langle Se(2)–O\rangle$ = *1.698*; $\langle O–Se(2)–O\rangle$ = 101.9

H	O(h)	O(3)	O(3)
O(h)	*0.962(61)*	3.312(3)	3.312(3)
O(3)	132.4(22)	*2.585(46)*	3.521(4)
O(3)	132.4(22)	85.8(28)	*2.585(46)*

RESULTS AND DISCUSSION

Crystal Structure

Relevant interatomic distances and bond angles in $NaCo_2(SeO_3)_2(OH)$ as well as the distortion parameters Δ_{oct} and σ^2_{oct} for the CoO_6 polyhedra are listed in Table 3. The results of bond valence calculations, neglecting the hydrogen atom, are given in Table 4. Figure 1 shows the atomic arrangement in a projection on (001). The crystal structure of $NaCo_2(SeO_3)_2(OH)$ is build up from two crystallographically distinct pyramidal SeO_3 groups, two different CoO_6 octahedra, one type of [4 + 2]-coordinated sodium atoms, and the hydrogen atom of an OH group which belongs to the CoO_6 octahedra. All atoms are located on the mirror planes except Co(1) with point symmetry $\bar{1}$, and O(3) and O(4), occupying general positions.

TABLE 4
Bond Valence Calculations According to (30) for $NaCo_2(SeO_3)_2(OH)$

ν(vu)	$Na^{[4]}$	Co(1)	Co(2)	Se(1)	Se(2)	Σ
O(1)	0.24↓→	0.31↓↓→→		1.28↓→		2.14
O(2)	0.26↓→		0.37↓→		1.42↓→	2.05
O(3)	0.26↓↓→		0.27↓↓→	1.36↓↓→		1.89
O(4)		0.31↓↓→	0.29↓↓→		1.33↓↓→	1.93
O(h)		0.38↓↓→→	0.34↓→			1.10
Σ	1.02	2.00	1.83	4.00	4.08	

Note. The hydrogen atom and the two longer Na–O bonds are not considered in the calculations.

The selenium atoms are one-sided coordinated to three oxygen atoms, a configuration which is typically caused by the activity of the lone-pair electrons of Se(IV) atoms. The shapes of both SeO_3 groups agree well with data found for other selenite compounds and with average values compiled in the literature (e.g., 5, 19). A noticeable deviation from the ideal values is a short edge within the $Se(1)O_3$ group [O(3)–O(3) = 2.521 Å], which is shared with the $Co(2)O_6$ polyhedron.

The CoO_6 polyhedra are more evidently distorted from an ideal octahedral shape. Co(1) is coordinated to four nearly equidistant oxygen atoms and two closer OH groups, forming a compressed pseudotetragonal dipyramid. The $Co(2)O_6$ polyhedron is more irregularly distorted, but may also be described as compressed, namely along its O(2)–O(h) axis. Generally, individual and mean Co–O distances as well as bond length and angular distortion parameters are in a range commonly found for CoO_6 polyhedra (20). In $NaCo_2(SeO_3)_2(OH)$ the CoO_6 polyhedra are linked by common edges forming $^1_\infty[Co_4O_{14}]^{20-}$ zigzag chains, which are comparable in topology and symmetry with those found in the α-olivine structure type $Me(II)^{[6]}_2SiO_4$: centric $Co(1)O_6$ groups constitute the straight part of the chains [common edges: O(1)–O(h) = 2.795 Å 2×; Co(1)–Co(1) = 3.021 Å 2×], whereas slightly larger $Co(2)O_6$ groups (symmetry *m*) form the zig and zag branches [common edges with $Co(1)O_6$: O(4)–O(h) = 2.722 Å 2×; Co(1)–Co(2) = 3.206 Å 2×]. In both structure types these chains extend along the *c* axis, leading to similar values for this cell edge [6.00 Å in α-Co_2SiO_4 (21, 22)]. While in the α-olivine structure individual chains are interconnected by common corners, in $NaCo_2(SeO_3)_2(OH)$ they are linked via the selenite groups and sodium atoms (Fig. 2); the contribution of the hydrogen bonds to this linkage is assumed to be negligible (see below).

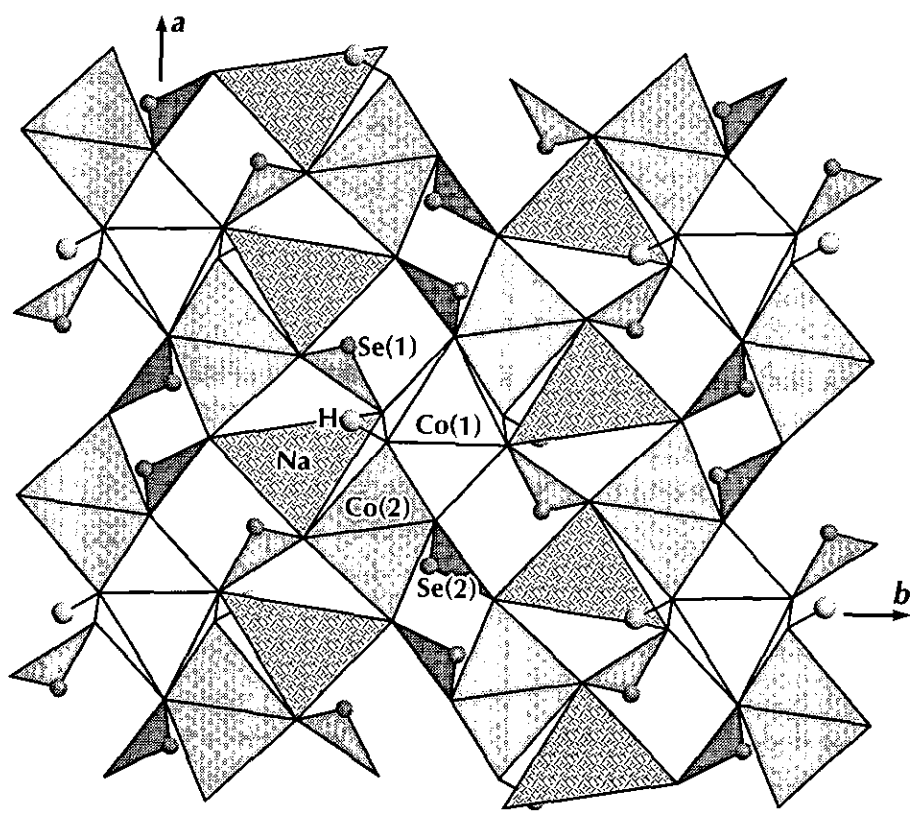

FIG. 1. Projection of the crystal structure of $NaCo_2(SeO_3)_2(OH)$ along *c*.

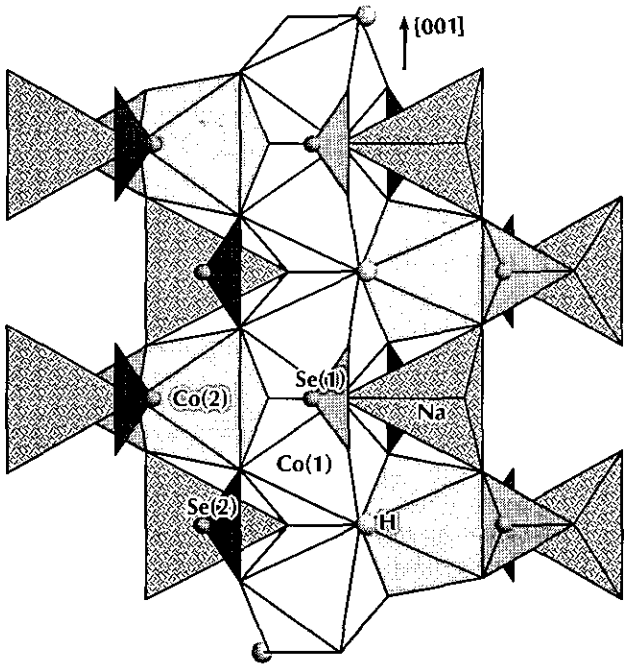

FIG. 2. Projection of the crystal structure of $NaCo_2(SeO_3)_2(OH)$ on (120), showing a $^1_\infty[Co_4O_{14}]^{20-}$ chain with all adjacent H atoms, NaO_4, and SeO_3 polyhedra.

The Na atom is coordinated to four oxygen atoms in a distorted tetrahedral arrangement. The NaO_4 polyhedron shares an O(1) and two O(3) corners within one $^1_\infty[Co_4O_{14}]^{20-}$ chain and an O(2) corner with a neighboring chain. The mean Na–O bond length of 2.308 Å is in agreement with crystal chemical expectations for $Na^{[4]}$–O bonds. The Na–O distances of two further O(3) atoms are longer by ~29% and the resulting mean $Na^{[6]}$–O distance of 2.531 Å is clearly longer than corresponding data given in the literature [e.g., 2.44 Å in (23)]. This fact as well as the bond valence calculations for the Na atom (Table 4) indicate that the contribution of the two additional O(3) atoms to the charge compensation of the Na atom is very small.

The oxygen atom of the hydroxyl group, O(h), belongs to three CoO_6 polyhedra: it is one-sided pyramidally coordinated to two Co(1) and one Co(2) atom with a bond valence sum of only 1.10 vu (Table 4), a value which typically reveals an oxygen donor of a hydroxyl group. The H atom completes the coordination of O(h) by forming the apex of a distorted trigonal pyramid. Formally, a bifurcated hydrogen bond with two symmetrically equivalent O(3) atoms as acceptors may be proposed, however, judging from the hydrogen bond length [O(h) ··· O(3) = 3.312 Å 2×], a practically free hydroxyl group with very weak H ··· O(3) interactions is indicated (but see below). Hence, the small deficiency in the bond valence sum for O(3) (Table 4, calculated without the H atom) should not be assigned exclusively to hydrogen bonding. A contribution of the long Na–O(3) bond (see above) and general uncertainties inherent in the empirical bond valence method have to be considered, too.

The environments of the oxygen atoms O(1) to O(4) can also be gathered from an inspection of Table 4. The corresponding configurations are: a distorted tetrahedron around O(1), a planar [3]-coordination of O(2), and pyramidal [3]-coordinations of O(3) and O(4) (bond angle sums 327.5° and 349.4°, respectively). Considering the long Na–O(3) distance and also the hydrogen atom for the environment of O(3), the corresponding configurations are a flat disphenoidal [4]-coordination and a pyramidal [5]-coordination, respectively.

Polarized Electronic Absorption Spectra

Figure 3 shows the polarized absorption spectra of $NaCo_2(SeO_3)_2(OH)$ in the range from 4000 to 34,000 cm^{-1}. The three distinct regions of absorption, observed around 6500, 13,400, and 19,000 cm^{-1}, are clearly correlated with the presence of d^7 configurated high-spin Co^{2+} ions in octahedral (O_h) or pseudooctahedral oxygen ligand fields. The major contribution to absorption intensity is associated with spin-allowed electric dipole transitions from the Co^{2+} ground state in crystal fields, which is derived from the ^4F free ion term, to excited levels with parental ^4F or ^4P term. Assuming O_h symmetry in the first instance, the band system at ~6500 cm^{-1} is assigned to the $^4T_{1g}(F) \rightarrow {}^4T_{2g}(F)$ transition. Within this band system, the first overtone of the OH stretching vibration is observed as a very weak, sharp feature at 6925 cm^{-1}. This position reveals significant hydrogen bonding, contrary to the interpretation drawn from the long O–H ··· O distance found in the crystal structure determination. This discrepancy may be attributed to the bifurcation of the hydrogen bond, which leads to a low-frequency shift of the OH streching vibrations (e.g., 24). The $^4T_{1g}(F) \rightarrow {}^4A_{2g}(F)$ transition is depicted in the strong field limit as a two electron jump ($t_2^5e^2 \rightarrow t_2^3e^4$), which has very low probability (e.g., 25). Its energy is expected to be approximately twice that of the first spin-allowed transition (26). Consequently, the weak and broad peak at ≈13,400 cm^{-1} is undoubtedly assigned to $^4T_{1g}(F) \rightarrow {}^4A_{2g}(F)$. The intensity of the prominent band system spanning the spectral region from ~16,000 to 22,000 cm^{-1} is predominantly ascribed to the spin-allowed $^4T_{1g}(F) \rightarrow {}^4T_{1g}(P)$ transition, but a significant contribution of intensity enhanced spin-forbidden quartet → doublet transitions is assumed. Above 23,000 cm^{-1} only very weak spectral features are observed, obviously due to further spin-forbidden transitions. The UV absorption edges occur at ~34,000 cm^{-1} and are nearly polarization independent.

The strong polarization of the bands as well as the

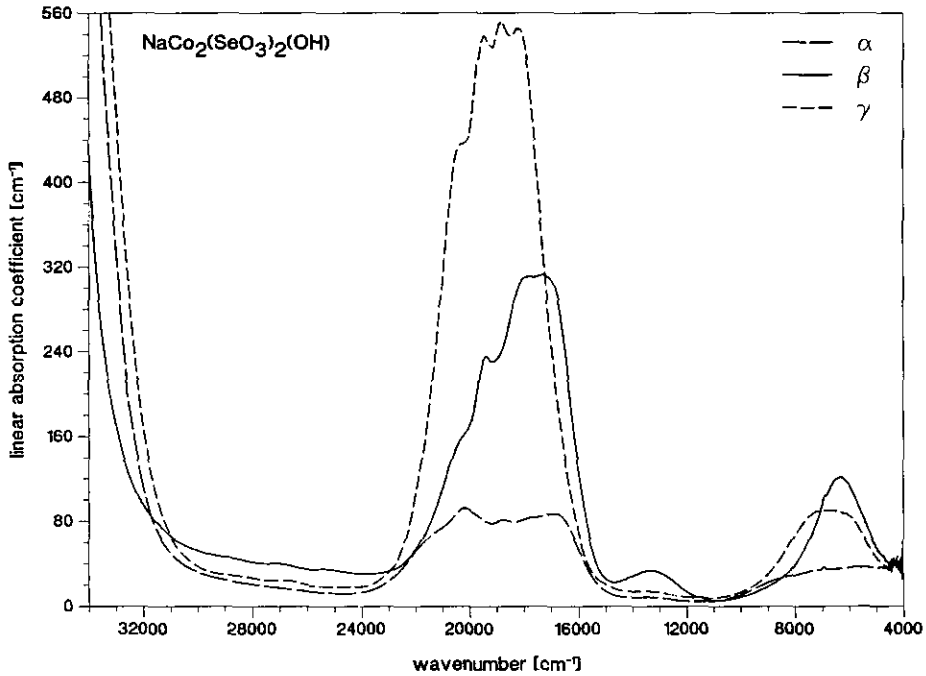

FIG. 3. Polarized absorption spectra of $NaCo_2(SeO_3)_2(OH)$ in the region from 4000 to 34,000 cm^{-1}.

structure and considerable width of the $^4T_{2g}(F)$ and $^4T_{1g}(P)$ bands indicate that degenerate energy levels are split in $NaCo_2(SeO_3)_2(OH)$ and a discussion in terms of O_h symmetry is not appropriate. Since the actual symmetries of the CoO_6 octahedra, C_i and C_s, are not very useful for the interpretation of the polarization depencencies (but see below), higher pseudosymmetries have to be modeled. Recalling the above discussion of the crystal structure, this is quite straightforward for the centric Co(1)O_6 polyhedron, which rather closely approaches D_{4h} symmetry. The pseudotetragonal axis of compression is the O(h)–O(h) axis, which is approximately perpendicular to the a cell edge (81.2°). The angles with b and c are 48.9° and 42.5°, respectively. The Co(2)O_6 polyhedron lacks a center of symmetry and has a stronger bond angle distortion, but may, in a first approximation, also be considered as tetragonally compressed along the O(2)–O(h) axis. This O(2)–O(h) direction lies in the ab plane and is nearly parallel with a (2.4°).

The static absence of an inversion center at the Co(2) site enables d–d electron transitions, whereas transitions at the centric Co(1) sites are Laporte-forbidden and may only gain comparatively low intensities through uneven octahedral vibrations (T_{1u} and T_{2u}), dynamically removing the center of symmetry. Hence, the intense absorptions in the β and γ spectra are attributed to cobalt at the Co(2) sites, while the weak α spectrum is probably dominated by transitions at the Co(1) sites. In descending from O_h to acentric tetragonal subgroups, degenerate T_{1g} and T_{2g} levels are split into $A_{(2)} + E$ and $B_{(2)} + E$, respectively, and $A_{2g}(O_h)$ transforms as $B_{(1)}$. The components of the electric dipole moment operator transform as $A_2 + E$ (in D_4), $A_1 + E$ (C_{4v}), and $A + E$ (in C_4) when the electric vector is aligned parallel ($\parallel$) and perpendicular ($\perp$) to the fourfold axis, respectively. An inspection of the corresponding symmetry selection rules reveals that the polarization behavior can be roughly explained assuming D_4 as pseudosymmetry for the Co(2) site and the $^4A_2$ split component as the ground state (Fig. 4). Only in that

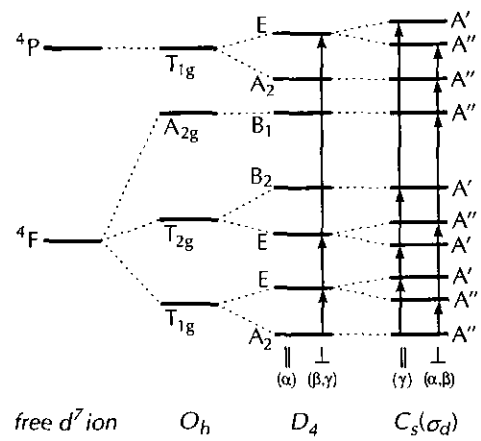

FIG. 4. Schematic crystal field splitting diagram $O_h \rightarrow D_4 \rightarrow C_s(\sigma_d)$ and corresponding symmetry selection rules for spectroscopic quartet states of Co^{2+} ions at the acentric Co(2) sites.

case all transitions are symmetry forbidden in ∥ orientation, i.e., in the α spectrum. On the other hand, in contradiction to the observed band splittings in β and γ, only $A_2 \rightarrow E$ transitions are allowed in ⊥ orientation. Obviously, the actual symmetry at the Co(2) site, C_s, has to be considered as substantial perturbation of the corresponding crystal field. In C_s all orbital degeneracies are removed, leading to A' and A'' split levels as shown in Fig. 4 for the appropriate subgroup orientation $C_s(\sigma_d)$. According to the symmetry selection rules, transitions from the new ground state A'' to A' levels are allowed in ∥ orientation, $A'' \rightarrow A''$ transitions in ⊥ orientation. Considering that ∥ and ⊥ refer to the electronic z axis, i.e., to the direction perpendicular to the mirror plane, the analogies $\parallel \equiv \gamma$ and $\perp \equiv \alpha, \beta$ are established and the intense β and γ spectra may be interpreted as follows: in the NIR region, the rather symmetrically shaped band in β polarization centered at 6310 cm^{-1} represents an $^4A'' \rightarrow {}^4A''$ transition. In the γ spectrum, two transitions to $^4A'$ levels at ~6000 and ~7200 cm^{-1} give rise to a broad composite band. The low energy levels around 6200 cm^{-1} are split components of the ^4E state in tetragonal approximation, while the energetically higher $^4A'$ level corresponds to tetragonal $^4B_2$. As mentioned above, the first overtone of the OH stretching vibration occurs at 6925 cm^{-1} in the β (and also α) spectrum, but is absent in γ. This behavior is in accordance with the OH dipole orientation found in the crystal structure determination. The weak two-electron jump $^4A'' \rightarrow {}^4A''$, equivalent to the $^4T_{1g} \rightarrow {}^4A_{2g}$ transition in O_h, is symmetrically forbidden in γ polarization, but allowed in the β spectrum, where it is located at 13,350 cm^{-1}. As a consequence of spin–orbit coupling, the prominent band system in the VIS region is obviously complicated by further splitting of spin-allowed transitions as well as by intensity enhancement of nearby spin-forbidden doublet states due to admixture of some quartet character. Distinct maxima or shoulders are observed at 17,300 (β), 17,900 (β), 18,200 (γ), 18,820 (γ), 19,390 (β), 19,460 (γ), and ~20,300 cm^{-1} (β, γ). The spectral features on the high energy side near 19,400 and at ~20,300 cm^{-1} are assigned to spin-forbidden transitions to components of $^2T_{1g}(O_h)$, derived from the ^2P free ion term, and to $^2A_{1g}(O_h)$, with parental ^2G term, respectively. The $^2T_{1g}$ level is practically unaffected by the strength of the crystal field and thus occurs at similar positions in other comparable Co^{2+} compounds (e.g., 27). An assignment of the remaining band features to low symmetry components of the spin-allowed octahedral $^4T_{1g}(P)$ level is quite ambiguous. Generally, the $^4A'' \rightarrow {}^4A''$ transitions, which are symmetry allowed in β polarization, are apparently located at somewhat lower energies than the γ polarized $A'' \rightarrow A'$ transition. In the UV region the β and γ spectra exhibit only very weak and broad bands centered at ~25,400 (β), ~26,900 (β, γ), and ~28,500 cm^{-1} (β, γ). They are probably correlated with spin-forbidden transitions to the octahedral $^2E(H)$, $^2T_{2g}(D_2)$, and $^2T_{1g}(H)$ levels.

TABLE 5

Observed[a] and Calculated Energy Levels (cm^{-1}) (Tetragonal Approximation) for the Co(2) Site in $NaCo_2(SeO_3)_2(OH)$ and Respective Tetragonal and Octahedral Assignments with Parental Free Ion Terms in Parentheses. Corresponding Crystal Field Parameters are $Dq = 630$, $Dt = -135$, $Ds = -111$, $B = 843$, $C = 3520$ cm^{-1}

Observed[a]	Calculated	D_4^b	O_h
—	0	$^4A_2$	$^4T_{1g}(^4F)$
—	352	^4E	
6150[a]	5963	^4E	$^4T_{2g}(^4F)$
7200	7158	$^4B_2$	
—	9275,10267		$^2E(^2G)$
13350	13458	$^4B_1$	$^4A_{2g}(^4F)$
—	14616,15094 15327,15950		$^2T_{1g}, {}^2T_{2g}(^2G)$
17600[a]	17738	$^4A_2$	$^4T_{1g}(^4P)$
18400[a]	18239	^4E	
19390	19339	$^2A_2$	$^2T_{1g}(^2P)$
19460	19545	^2E	
20300	20168	$^2A_1$	$^2A_{1g}(^2G)$
—	22531,23091 23310,24136		$^2T_{1g}, {}^2T_{2g}(^2G)$
25400	25230	$^2B_1$	$^2E_g(^2H)$
	25447	$^2A_1$	
26900	27743	^2E	$^2T_{2g}(^2D_2)$
	27895	$^2B_2$	
28500	28558	$^2A_2$	$^2T_{1g}(^2H)$
	28849	^2E	

Note. Calculations are based on transition energies observed in the β and γ spectra.

[a] Averaged observed energies used for the tetragonal calculation.

[b] Unobserved spin-forbidden levels: only the O_h representation is given.

An interpretation of the weak α spectrum in terms of Laporte-forbidden transitions within the centric $Co(1)O_6$ polyhedra is seriously complicated by the fact that the contribution of Co(2) transitions to the α spectrum can hardly be estimated. At least it can be stated that, in accordance with the shorter mean Co(1)–O distance and the resulting higher crystal field strength at the Co(1) site, the α spectrum exhibits high energy components in the region of the NIR and VIS band system (shoulders at ~8800 and ~21,300 cm^{-1}, respectively), which are not observed in the β and γ spectra.

The above-mentioned uncertainties in the band assignments make quantitative crystal field calculations rather difficult. Nevertheless, for the Co(2) site a treatment in terms of the tetragonal crystal field parameters Dq, Dt, Ds, and the Racah parameters B and C may perhaps yield some reliable results. The selection of input values for the least-squares fit of Dq, Dt, Ds, and B to the spin-allowed transitions is clear for the low energy F states, i.e., $^4A_2$ as ground state, tetragonally nondegenerate levels as observed ($^4B_2$, 7200 and $^4B_1$, 13,350 cm^{-1}), and 6150 cm^{-1} as approximate center of gravity of the NIR ^4E level. The positions of the $^4A_2(P)$ and $^4E(P)$ levels are only roughly estimated to be somewhere around 17,600 and 18,400 cm^{-1}, respectively. If the latter two are weighted only half in the fitting process, the following parameters are obtained: $Dq = 630$, $Dt = -135$, $Ds = -111$, and $B = 843$ cm^{-1} (Dt and Ds sign convention according to Ref. 17). From the positions of the spin-forbidden $^2T_{1g}(P)$ and $^2A_{1g}(G)$ levels Racah C is estimated as ~3520 cm^{-1}. Table 5 compares calculated and observed energy levels and lists the corresponding assignments. Generally, the obtained crystal field parameters are in accordance with the expectations: in the crystal field, the Racah parameter B is reduced to 87% of its free ion value (971 cm^{-1}, Ref. 28), the C/B ratio is 4.18. From the relation between the fitted parameter Dq, which represents the equatorial field strength Dq(eq), and the tetragonal parameter Dt, an axial crystal field strength $Dq(ax) = 866$ cm^{-1} and an average (cubic) field strength $Dq(av) = 709$ cm^{-1} can be calculated. This value is somewhat low compared with cubic Dq values for other Co^{2+} selenites (27), ranging between 735 and 780 cm^{-1}. The negative sign of Dt is in agreement with the compressed geometry of the $Co(2)O_6$ polyhedron. The magnitude of Dt is also quite reliable since it depends, to first order, only on the splitting of the octahedral $^4T_{2g}(F)$ state. On the other hand, Ds mainly depends on the $^4T_{1g}(P)$ splitting and thus, its value may be considerably in error and even its sign cannot be stated definitely.

ACKNOWLEDGMENTS

The author thanks Doz. H. Effenberger, Professor F. Pertlik, Professor E. Tillmanns, and Professor J. Zemann, Vienna, for helpful discussions concerning the crystal structure of $NaCo_2(SeO_3)_2(OH)$. The investigation of the optical absorption spectra at the Technische Universität Berlin was made possible through a research fellowship, generously provided by the Alexander von Humboldt-Stiftung, Bonn, Bad Godesberg. Thanks are due to Professor K. Langer, Berlin, for many useful discussions, and M. Andrut, Berlin, for technical assistance. H. Reuff, Berlin, carefully prepared the samples for the spectroscopic measurements.

REFERENCES

1. K. Kohn, K. Inoue, O. Horie, and S. Akimoto, *J. Solid State Chem.* **18,** 27 (1976).
2. O. J. Lieder and G. Gattow, *Naturwissenschaften* **54,** 443 (1967).
3. M. Wildner, *N. Jb. Miner. Monatsh.* **1990,** 353 (1990).
4. M. Wildner, *Monatsh. Chem.* **122,** 585 (1991); Erratum, 1109 (1991).
5. F. C. Hawthorne, L. A. Groat, and T. S. Ercit, *Acta Crystallogr. Sect. C* **43,** 2042 (1987).
6. W. T. A. Harrison, A. V. P. McManus, and A. K. Cheetham, *Acta Crystallogr. Sect. C* **48,** 412 (1992).
7. M. Wildner, *Acta Crystallogr. Sect. C* **48,** 410 (1992).
8. M. Wildner, *Acta Crystallogr. Sect. C* **50,** 336 (1994).
9. M. Wildner, *Mineral. Petrol.* **48,** 215 (1993).
10. M. Wildner, *Z. Kristallogr.* **185,** 499 (1988).
11. "Crystal Data Determinative Tables" (J. D. H. Donnay and H. M. Ondik, Eds.), Vol. II. NBS & JCPDS, 1973.
12. "International Tables for X-ray Crystallography," Vol. IV. Kynoch Press, Birmingham, 1974.
13. Stoe & Cie, "STRUCSY. Structure System Program Package." Stoe & Cie, Darmstadt, 1984.
14. K. Langer and K. R. Fentrup, *J. Microsc.* **116,** 311 (1979).
15. L. Cemič, S. Grammenopoulou-Bilal, and K. Langer, *Ber. Bunsenges. Phys. Chem.* **90,** 654 (1986).
16. J. R. Perumareddi, *J. Phys. Chem.* **71,** 3144 (1967).
17. C. J. Ballhausen, "Introduction to Ligand Field Theory." McGraw–Hill, New York/San Francisco/Toronto/London, 1962.
18. Y. Y. Yeung and C. Rudowicz, *Comput. Chem.* **16,** 207 (1992).
19. R. Fischer and J. Zemann, "Handbook of Geochemistry," Vol. II3, p. 34A. Springer-Verlag, Berlin/Heidelberg/New York, 1974.
20. M. Wildner, *Z. Kristallogr.* **202,** 51 (1992).
21. N. Morimoto, M. Tokonami, M. Watanabe, and K. Koto, *Am. Mineral.* **59,** 475 (1974).
22. M. Miyake, H. Nakamura, H. Kojima, and F. Marumo, *Am. Mineral.* **72,** 594 (1987).
23. W. H. Baur, *in* "Structure and Bonding in Crystals" (M. O'Keeffe and A. Navrotsky, Eds.), Vol. II, pp. 31–52. Academic Press, New York, 1981.
24. K. Nakamoto, M. Margoshes, and R. E. Rundle, *J. Am. Chem. Soc.* **77,** 6480 (1955).
25. S. Koide, *Philos. Mag.* **4,** 243 (1959).
26. A. B. P. Lever and D. Odgen, *J. Chem. Soc. A* **1967,** 2041 (1967).
27. M. Wildner and K. Langer, *Phys. Chem. Miner.* **20,** 460 (1994).
28. Y. Tanabe and S. Sugano, *J. Phys. Soc. Jpn.* **9,** 766 (1954).
29. W. H. Zachariasen, *Acta Crystallogr.* **23,** 558 (1967).
30. I. D. Brown and D. Altermatt, *Acta Crystallogr. Sect. B* **41,** 244 (1985).